SUBMARINE TECHNOLOGY

STD-R-1071

THE ELECTRICAL PROPERTIES OF SEAWATER (INCLUDING CONDUCTIVITY RELAXATION)

JULY 1984

COASTAL SCIENCE PROGRAM

STD-R-1071
THE ELECTRICAL PROPERTIES OF SEAWATER (INCLUDING CONDUCTIVITY RELAXATION)

JULY 1984

M. E. THOMAS

APPROVED FOR PUBLIC RELEASE,
DISTRIBUTION UNLIMITED

FINAL REPORT
TASK - ZEDO
CONTRACT - N00024-83-C-5301

SUBMARINE TECHNOLOGY DEPARTMENT
The Johns Hopkins University
Applied Physics Laboratory

UNCLASSIFIED
SECURITY CLASSIFICATION OF THIS PAGE

REPORT DOCUMENTATION PAGE

1a. REPORT SECURITY CLASSIFICATION Unclassified	1b. RESTRICTIVE MARKINGS
2a. SECURITY CLASSIFICATION AUTHORITY	3. DISTRIBUTION/AVAILABILITY OF REPORT
2b. DECLASSIFICATION/DOWNGRADING SCHEDULE	
4. PERFORMING ORGANIZATION REPORT NUMBER(S) STD-R-1071	5. MONITORING ORGANIZATION REPORT NUMBER(S)
6a. NAME OF PERFORMING ORGANIZATION Applied Physics Lab Johns Hopkins University 6b. OFFICE SYMBOL (If applicable)	7a. NAME OF MONITORING ORGANIZATION Office of Naval Research, Code 422CS
6c. ADDRESS (City, State, and ZIP Code) Johns Hopkins Road Laurel, MD 20707	7b. ADDRESS (City, State, and ZIP Code) Arlington, VA 22218
8a. NAME OF FUNDING/SPONSORING ORGANIZATION ONR 8b. OFFICE SYMBOL (If applicable) Code 420	9. PROCUREMENT INSTRUMENT IDENTIFICATION NUMBER
8c. ADDRESS (City, State, and ZIP Code) Arlington, VA 22218	10. SOURCE OF FUNDING NUMBERS PROGRAM ELEMENT NO. / PROJECT NO. / TASK NO. / WORK UNIT ACCESSION NO.

11. TITLE (Include Security Classification)
The Electrical Properties of Seawater (Including Conductivity Relaxation)

12. PERSONAL AUTHOR(S) M. E. Thomas

13a. TYPE OF REPORT	13b. TIME COVERED	14. DATE OF REPORT (Year, Month, Day)	15. PAGE COUNT
Technical Report	FROM 10/83 TO 9/84	1984, July	34

16. SUPPLEMENTARY NOTATION
Approved for Public Release, Distribution Unlimited

17. COSATI CODES		
FIELD	GROUP	SUB-GROUP

18. SUBJECT TERMS (Continue on reverse if necessary and identify by block number)
(a) Dielectrical Properties above one GHz (c) Conductivity Relaxation
(b) Seawater (d) Microwave

19. ABSTRACT (Continue on reverse if necessary and identify by block number)

The electrical properties of seawater for ac currents or fields of 1 GHz or higher frequencies are examined with particular emphasis on the effects of relaxation of the charge carriers with the frequency of the applied field. Such effects have not been definitively quantified either experimentally or theoretically. New experiments are conducted but are not conclusive. It is possible that the conductivity relaxation time is similar to the Debye relaxation time making direct observations of this effect difficult.

20. DISTRIBUTION/AVAILABILITY OF ABSTRACT	21. ABSTRACT SECURITY CLASSIFICATION
☒ UNCLASSIFIED/UNLIMITED ☐ SAME AS RPT. ☐ DTIC USERS	Unclassifed
22a. NAME OF RESPONSIBLE INDIVIDUAL W. M. Chambers	22b. TELEPHONE (Include Area Code) 301/953-5123 / 22c. OFFICE SYMBOL n/a

DD FORM 1473, 84 MAR 83 APR edition may be used until exhausted. All other editions are obsolete.

SECURITY CLASSIFICATION OF THIS PAGE
UNCLASSIFIED

The Johns Hopkins University
APPLIED PHYSICS LABORATORY
Laurel, Maryland

TABLE OF CONTENTS

The Johns Hopkins University
APPLIED PHYSICS LABORATORY
Laurel, Maryland

LIST OF ILLUSTRATIONS

LIST OF TABLES

The Johns Hopkins University
APPLIED PHYSICS LABORATORY
Laurel, Maryland

1. INTRODUCTION

A better understanding of the electromagnetic properties of aqueous electrolytes has important implications for oceanography and biology. The purpose of this study is to consider the conductivity relaxation time of seawater. Potentially, this phenomenon influences the electrical properties of seawater above 5GHz. Also, the dielectric resonant bands in the far-infrared affect the electrical properties beyond 5 GHz, and their effects are considered based on available information in the literature.

Although the study of aqueous electrolytic solutions has a long history, much yet remains to be understood. Essentially, the electrical properties of solutions of high concentration [>0.1 Molarity (M)] (i.e., seawater) are not completely understood and are typically represented by empirical models. To improve the present understanding of seawater conductivity, the determination of its relaxation time is important because it gives information about the mobility of the charge carriers.

To see how the properties of mobility influence the impedance of electrolytes, consider the standard definition for conductivity (Reference 1)

$$\sigma = \sum_{i=1}^{N} \left(|e_{+i}| n_{+i} \mu_{+i} + |e_{-i}| n_{-i} \mu_{-i} \right); \quad \sum_{i=1}^{N} \left(e_{+i} n_{+i} + e_{-i} n_{-i} \right) = 0 \tag{1}$$

where $n_{+,-i}$ is the number density of the ith +,- charge carrier, $e_{+,-i}$ is the charge of the ith +,- charge carrier, $\mu_{+,-i}$ is the carrier mobility of the ith +,- charge carrier, and N is the number of solutes. Since most electrolytes composing the ocean are 1:1, it is assumed that

$$|e_{+i}| n_{+i} = |e_{-i}| n_{-i} = \rho_i$$

The Johns Hopkins University
APPLIED PHYSICS LABORATORY
Laurel, Maryland

The conductivity for a single 1:1 solute simplifies to

$$\sigma = \rho(\mu_+ + \mu_-) . \tag{2}$$

A simple expression for the carrier mobility can be obtained from the following equations (Reference 2)

$$\mu = \frac{\langle v \rangle}{E}$$

and

$$m \frac{d\langle v \rangle}{dt} + mg \langle v \rangle = eE . \tag{3}$$

where $\langle v \rangle$ is the mean velocity of the charge carrier, m is the mass, g is the damping constant, e is the charge of the charge carrier, and E is the applied electric field. Let $\langle v \rangle$ and E be time harmonic as $e^{j\omega t}$. The solution of Equation (3) results in the following

$$\mu = \frac{\mu_o}{1 + j \frac{\omega}{g}} \; ; \; \mu_o = \frac{e}{mg} . \tag{4}$$

Substituting this result into Equation (2), the conductivity becomes

$$\sigma = \rho \left[\frac{\mu_{o+}}{1 + j \frac{\omega}{g_+}} + \frac{\mu_{o-}}{1 + j \frac{\omega}{g_-}} \right] . \tag{5}$$

It is assumed that the damping forces will be similar for both the positive and negative charge carriers. Therefore,

$$g_+ = g_- = g .$$

The "g" parameter is the reciprocal of the conductivity relaxation time. This interpretation is easily seen from Equation (3). When the applied E-field is turned off, the charge carriers relax back to equilibrium and the mean velocity becomes

$$\langle v \rangle = \langle v(t=0) \rangle \, e^{-tg} \quad .$$

The conductivity relaxation time, $1/g$, is designated "τ_c." Thus,

$$\sigma = \rho(\mu_{o+} + \mu_{o-}) \; \frac{1}{1 + j \frac{\omega}{g}}$$

$$= \sigma_o \frac{1}{1 + j\omega\tau_c} \quad .$$

where τ_c is the conductivity relaxation time related to mobility. The factor σ_o represents the conductivity according to the Debye-Falkenhagen theory (Reference 3) and the remaining factor represents the correction for inertia.

The impedance can now be determined for a parallel plate probe as

$$Z = \frac{\ell}{A\sigma} - j\,\frac{1}{\omega C} = \frac{\ell}{A\sigma}\left(1 + j\,\frac{\omega}{g}\right) - j\,\frac{1}{\omega C} \qquad (7)$$

$$= R_o + j\left(\omega L - \frac{1}{\omega C}\right) \; ; \; L = \frac{\ell}{A\sigma g} = \frac{R_o}{g}$$

where ℓ is the length of the sample and A is the cross-sectional area of the plate. R_o is the DC resistance, L is the effective inductance, and C is the capacitance of the solution between the plates. Since the ions cannot move instantaneously with the applied field, the current will lag the voltage. The conductivity relaxation time, τ_c, is determined by computing L/R_o.

Impedance measurements of this type should be used instead of microwave cavity measurements, which are influenced by both the conductive and dielectric properties of the measured medium. By keeping the frequency of the applied field low enough (< 1 GHz) so that the real part of the dielectric constant is constant, the imaginary part is very small and the conductivity high enough so that the capacitive (i.e., dielectric) character is shorted out; then measurement can readily be made. The main problem remaining is minimizing the stray capacitance and residual inductance.

Section 2 describes the impedance experiment designed to measure the conductivity relaxation time of seawater and related electrolytes. Section 3 reviews the present model used for describing the electrical properties of seawater and discusses the effect of conductivity relaxation and other mechanisms on this model.

2. ELECTRICAL IMPEDANCE MEASUREMENTS

The major thrust of this project is to measure the electrical impedance of seawater-related electrolytes. A special conductivity cell was designed and constructed for this purpose. The following describes the experimental apparatus used and presents the results of the experiment.

2.1 Experimental Apparatus

Figure 1 illustrates the experimental apparatus. The impedance measurements were made with a Hewlett-Packard (HP) multifrequency LCR meter model number 4275A, which operates at ten different frequencies between 10 kHz and 10 MHz. The LCR meter was computer controlled by an HP 9845A computer. A conductivity test cell was connected to the LCR meter in such a way that the shields of the 4-terminal network were connected to the shield enclosing the test cell. As shown in Figure 1, the current passing through the cell also was carried by the shield thus canceling the magnetic field generated by the central conductor. This reduced the residual inductance of the network.

Figure 2 shows the unique design of the modified Jones cell that was used as the test cell. The cell can be filled and drained without disconnecting it from the LCR meter. Also, the cell can be temperature controlled by an external bath. The cell constant is 17.2 ($\pm$0.15)cm^{-1}. The temperature of the cell is monitored by placing a probe inside a well in contact with the circulating bath.

The accuracy of the impedance measurements depends on the LCR meter and background effects of the test cell. The LCR meter does open- and short-circuit measurements of the test network and measures the stray capacitance and residual inductance. The values are stored and then subtracted from the actual measurements. The open-circuit measurement is done with the cell empty. The short-circuit measurement is done with the cell filled with mercury. In this way, most of the stray capacitance and residual inductance are accounted for. Without this capability these measurements would not be possible. The LCR meter reduces the stray capacitance and the residual inductance to some nominal level. These levels are measured before every experiment. Figure 3 shows the accuracy of the magnitude and phase of the impedance.

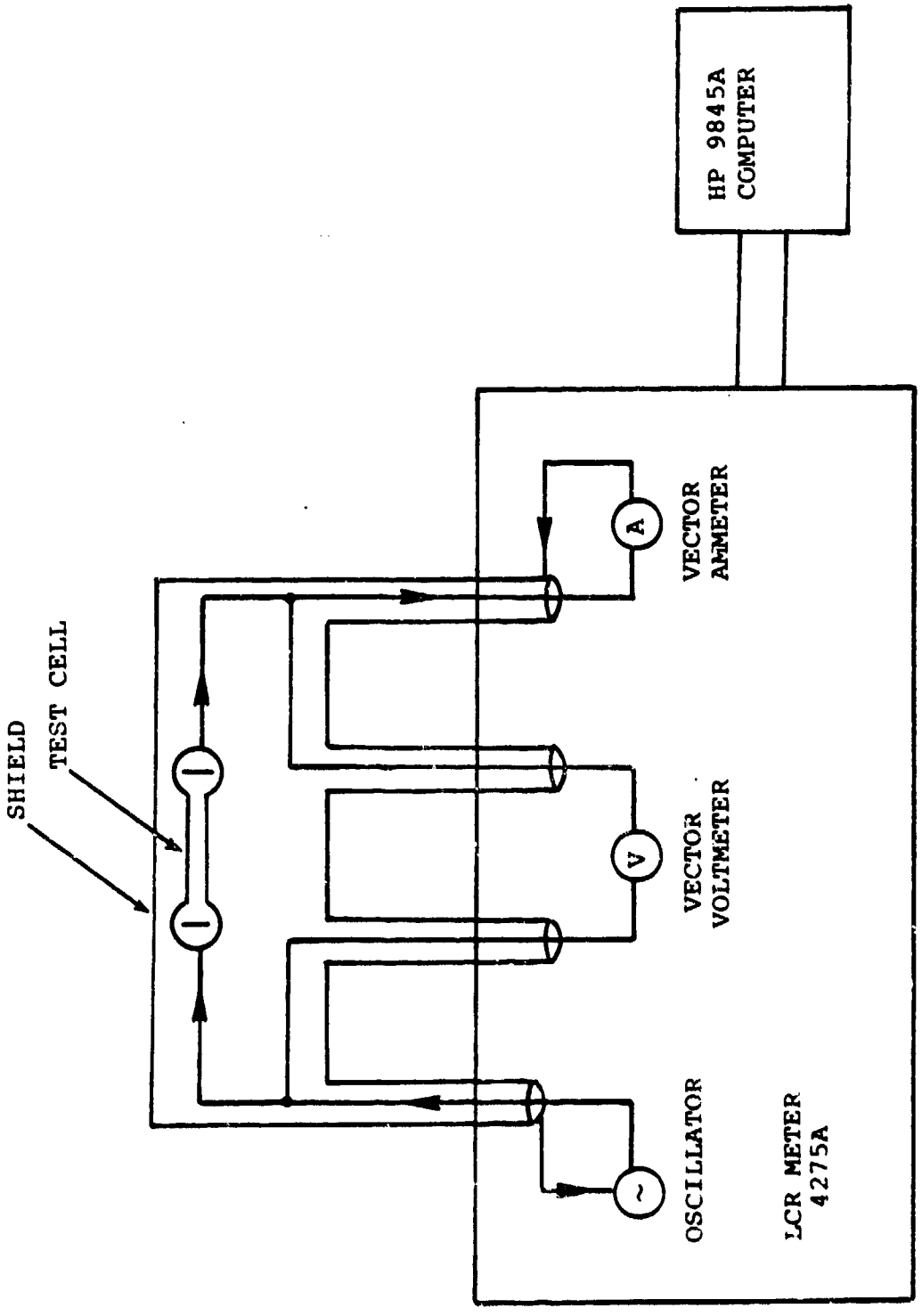

Figure 1 Experimental Apparatus (vector meters measure magnitude and phase)

The Johns Hopkins University
APPLIED PHYSICS LABORATORY
Laurel, Maryland

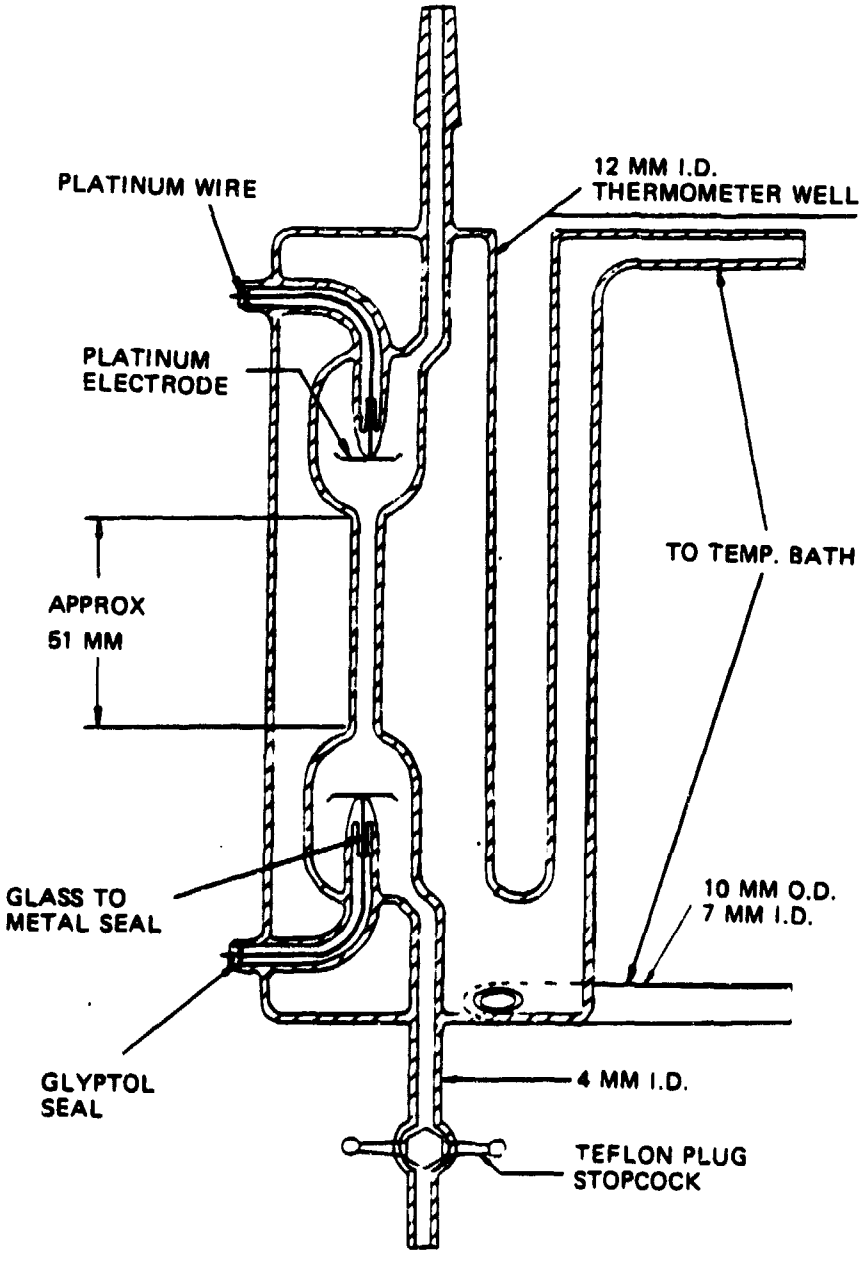

Figure 2 Modified Jones Test Cell

The Johns Hopkins University
APPLIED PHYSICS LABORATORY
Laurel, Maryland

|Z| - θ MEASUREMENT

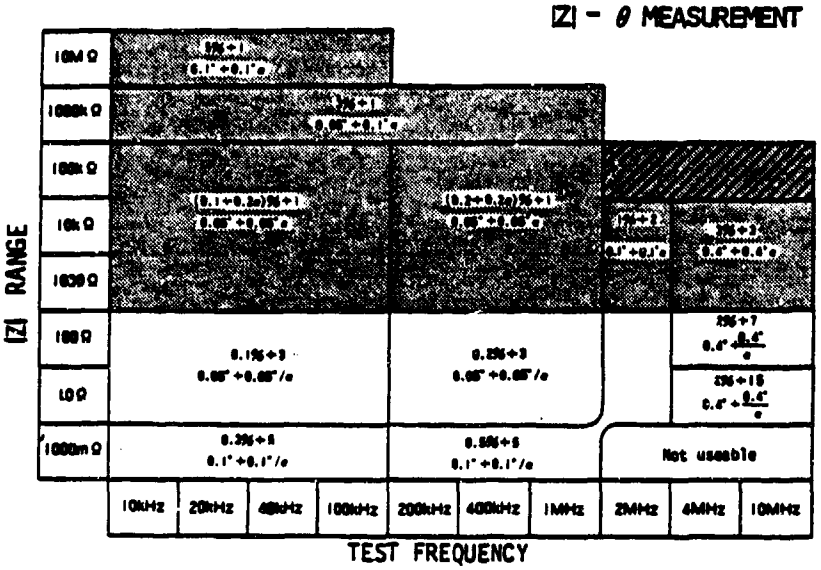

Equations in table represent:

Impedance accuracy
Phase angle accuracy

α, 1/α: See Figure A Accuracy Coefficient Graph.

θ measurement range:

-180.000° - +180.000°

Display counts for |Z| and θ (normal mode):

Ranges	|Z|	θ
	*36 - 1999	0 - 18000
	0 - 19999	0 - 18000

*Approximate value (unspecified).

Number of significant digits displayed for |Z| and θ depend on test signal level, range and frequency (5 digits max.).

Accuracies in lined areas ▨ are unspecified.

ACCURACY COEFFICIENTS

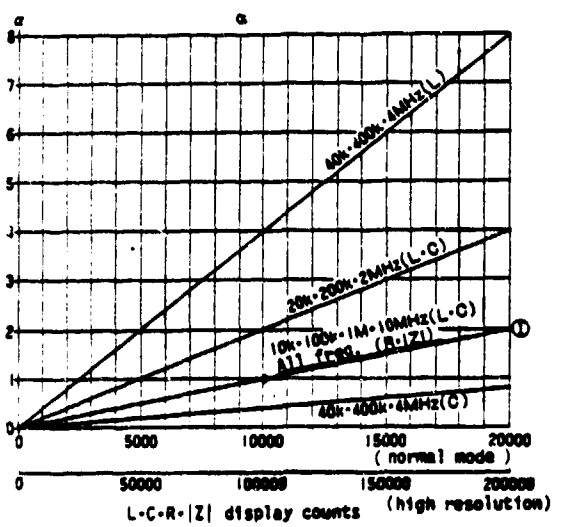

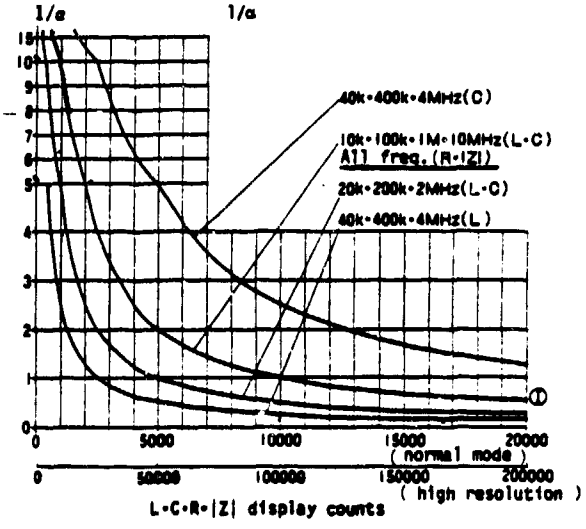

Figure 3 LCR Meter Accuracy

The test cell changes between the open and short circuit measurements and the actual measurement of electrolytic solutions. This is because of the double-layer effect at each electrode and the difference in self-inductance between a good conductor (mercury) and a fair conductor (the electrolytic solutions). These effects cannot be nulled out by the LCR meter since they are not present during the open and short circuit tests. The double layer effect is caused by the electronic-to-ionic conductor interface. The result is the formation of a leaky capacitor at each electrode, as shown in Figure 4. Also, the self-inductance of the test cell is much larger for the electrolytic solutions than for mercury. Calculations for an infinitely long conductor indicate the difference to be around 5 nH. However, end effects will certainly increase this number.

2.2 Results

Measurements on carbon composition resistors were made to test the system background. Since the resistors are electronic conductors, the effects of conductivity relaxation will occur at frequencies much higher than ionic conductors. Two resistors were used, one with a resistance of 228Ω and the other with a resistance of 7570Ω. This range of values of resistance is close to those of the electrolytic solutions studied. Tables 1 and 2 list the results of the carbon composition resistors. The format is typical of all experimental results. Background measurements are made after the open- and short-circuit calibration measurements [a zero offset adjustment (ZOA)], separately. Thus, the stray capacitance and residual inductance of the network are recorded. The stray or parasitic background capacitance is measured at 40 kHz and the residual or parasitic background inductance is measured at 10 MHz. The measured background capacitance and inductance as listed are typically the meter's limit of sensitivity. The device to be measured is then connected to the test network and approximate values for the inductance and capacitance are

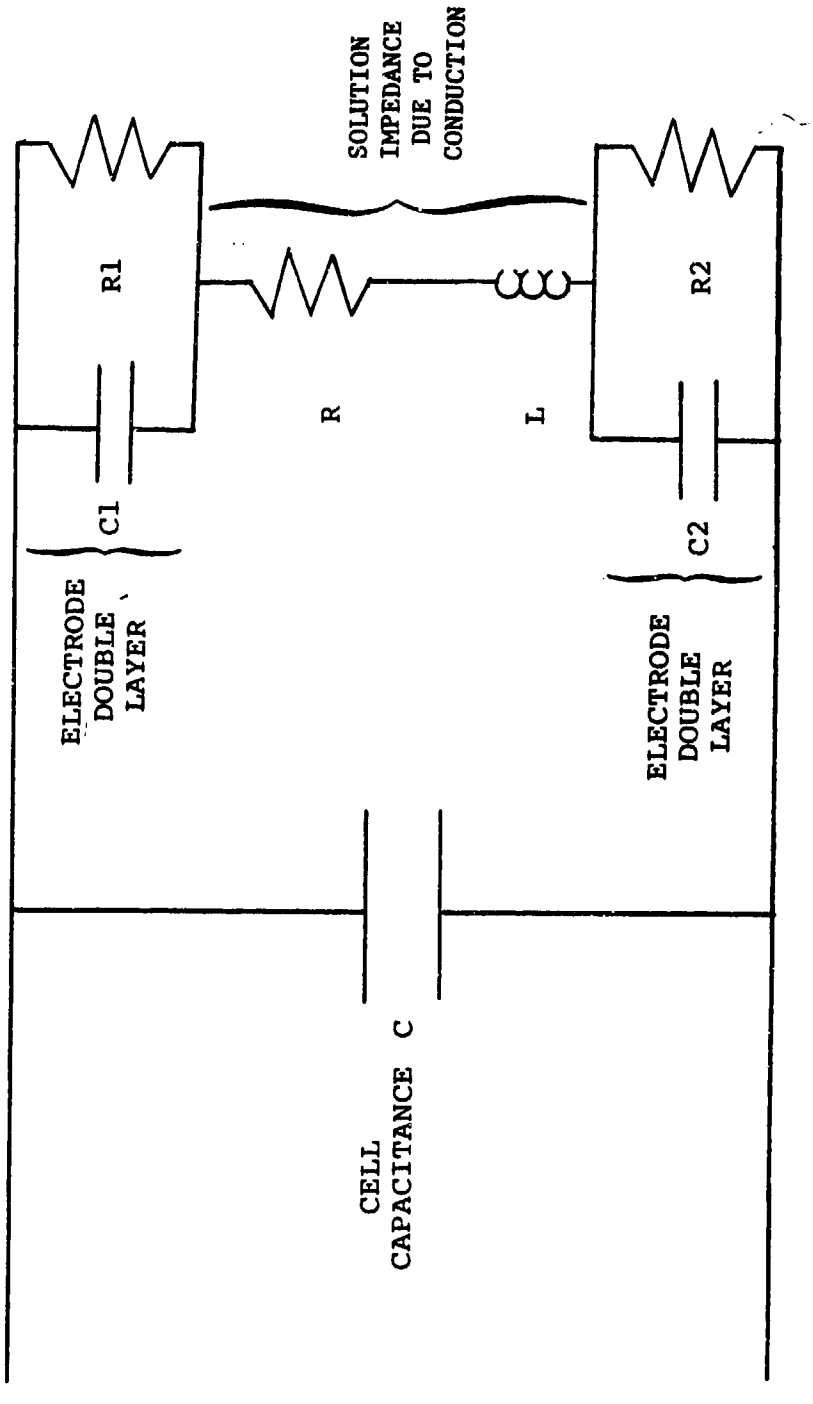

Figure 4 Equivalent Electrical Circuit

The Johns Hopkins University
APPLIED PHYSICS LABORATORY
Laurel, Maryland

Table 1

228Ω CARBON COMPOSITION RESISTOR RESULTS

02/09/84 16:30 CARBON COMP RESISTOR
KEY SETTINGS ARE A1B3C2D0F20H1I0M2R3180T1

FREQUENCY	PARASITIC BACKGROUND CAPACITANCE AND CONDUCTANCE	
40K	-2.160000000000E-16	.000000000012

FREQUENCY	PARASITIC BACKGROUND INDUCTANCE
10M	5.026000000000E-10

RESISTOR

APPROXIMATE INDUCTANCE
-.000000011086

CELL CAPACITANCE
2.000000000000E-14

			MEASURED IMPEDANCE		CORRECTED IMPEDANCE	
FREQUENCY	VOLTAGE	CURRENT	MAGNITUDE	PHASE	MAGNITUDE	PHASE
1.0E+04	2.40E-01	1.00E-03	2.2828E+02	+0.00	2.2828E+02	+0.00
2.0E+04	2.30E-01	1.00E-03	2.2830E+02	+0.01	2.2830E+02	+0.01
4.0E+04	2.30E-01	1.00E-03	2.2829E+02	+0.00	2.2829E+02	+0.00
1.0E+05	2.30E-01	1.00E-03	2.2830E+02	-0.00	2.2830E+02	-0.00
2.0E+05	2.30E-01	1.00E-03	2.2829E+02	+0.00	2.2829E+02	+0.00
4.0E+05	2.30E-01	1.00E-03	2.2825E+02	+0.01	2.2825E+02	+0.01
1.0E+06	2.30E-01	1.00E-03	2.2825E+02	-0.01	2.2825E+02	-0.01
2.0E+06	2.30E-01	1.00E-03	2.2820E+02	+0.02	2.2820E+02	+0.03
4.0E+06	2.30E-01	1.00E-03	2.2812E+02	+0.03	2.2812E+02	+0.03
1.0E+07	2.10E-01	9.00E-04	2.3046E+02	-0.18	2.3046E+02	-0.16

CHANGED VOLTAGE 16:35

APPROXIMATE INDUCTANCE
-.000000015718

CELL CAPACITANCE
1.400000000000E-13

			MEASURED IMPEDANCE		CORRECTED IMPEDANCE	
FREQUENCY	VOLTAGE	CURRENT	MAGNITUDE	PHASE	MAGNITUDE	PHASE
1.0E+04	2.30E-02	1.00E-04	2.2819E+02	+0.01	2.2819E+02	+0.01
2.0E+04	2.30E-02	1.00E-04	2.2823E+02	+0.01	2.2822E+02	+0.01
4.0E+04	2.30E-02	1.00E-04	2.2823E+02	+0.01	2.2823E+02	+0.01
1.0E+05	2.30E-02	1.00E-04	2.2824E+02	+0.00	2.2824E+02	+0.00
2.0E+05	2.30E-02	1.00E-04	2.2823E+02	+0.01	2.2823E+02	+0.01
4.0E+05	2.30E-02	1.00E-04	2.2819E+02	+0.02	2.2819E+02	+0.02
1.0E+06	2.30E-02	1.00E-04	2.2821E+02	-0.00	2.2821E+02	+0.01
2.0E+06	2.30E-02	1.00E-04	2.2815E+02	+0.01	2.2815E+02	+0.03
4.0E+06	2.20E-02	9.00E-05	2.2809E+02	+0.00	2.2809E+02	+0.05
1.0E+07	2.00E-02	8.00E-05	2.3056E+02	-0.28	2.3056E+02	-0.15

Table 2

7570Ω CARBON COMPOSITION RESISTOR RESULTS

02/09/84 16:04 CARBON COMP RESISTOR
ICY SETTINGS ARE A1B3C20F20H110M3R31S0T1

++

FREQUENCY	PARASITIC BACKGROUND CAPACITANCE AND CONDUCTANCE	
40K	-8.60000000000E-17	.000000000134

++

FREQUENCY	PARASITIC BACKGROUND INDUCTANCE
10M	-1.01580000000E-09

02/09/84 16:04 CARBON COMP RESISTOR

++

APPROXIMATE INDUCTANCE
-.00000137668

CELL CAPACITANCE
3.63600000000E-13

++

			MEASURED IMPEDANCE		CORRECTED IMPEDANCE	
FREQUENCY	VOLTAGE	CURRENT	MAGNITUDE	PHASE	MAGNITUDE	PHASE
1.0E+04	1.10E-01	0.00E+00	7.5687E+03	+0.04	7.5687E+03	+0.04
2.0E+04	1.10E-01	0.00E+00	7.5707E+03	+0.03	7.5707E+03	+0.05
4.0E+04	1.10E-01	0.00E+00	7.5714E+03	-0.00	7.5714E+03	+0.04
1.0E+05	1.10E-01	0.00E+00	7.5729E+03	-0.11	7.5729E+03	-0.31
2.0E+05	1.10E-01	0.00E+00	7.5701E+03	-0.14	7.5701E+03	+0.06
4.0E+05	1.10E-01	0.00E+00	7.5674E+03	-0.30	7.5675E+03	+0.10
1.0E+06	1.10E-01	0.00E+00	7.5619E+03	-0.84	7.5627E+03	+0.17
2.0E+06	1.10E-01	0.00E+00	7.5395E+03	-1.66	7.5425E+03	+0.35
4.0E+06	1.10E-01	0.00E+00	7.5048E+03	-3.19	7.5157E+03	+0.81
1.0E+07	1.00E-01	0.00E+00	7.4039E+03	-7.11	7.4525E+03	+2.70

The Johns Hopkins University
APPLIED PHYSICS LABORATORY
Laurel, Maryland

obtained. Then the computer directs the LCR meter to take impedance measurements at the ten available frequencies between 10 kHz and 10 MHz. In addition to the frequency and the magnitude and phase of the impedance, the computer lists the approximate applied voltage and current, and a corrected magnitude and phase impedance. The measured cell capacitance is removed from the measured impedance to give the corrected impedance. The cell capacitance in the case of the carbon composition resistors is the capacitance between the two metal contacts at opposite ends of the resistor. In the case of the modified Jones cell, it is typically the capacitance between the two spherical ends of the capillary tube. For the carbon composition resistors, the cell capacitance is very small (0.4 to 0.1 pF or less). The impedance of the carbon composition resistors is largely resistive with a small capacitive influence at the higher frequencies. Notice that the listed approximate inductance is negative. This means the impedance was actually capacitive and not inductive. Thus the LCR meter could not properly interpret the result.

Tables 3, 4, and 5 list the main results of the experiment. For sodium chloride and seawater solutions (concentrations are listed in parts per thousand of solute over solution by weight), the impedance is purely resistive within the accuracy of the LCR meter. The inductive effect at the higher frequencies is less than 0.1 percent. In Table 3, the cell capacitance dominates at all frequencies and only the corrected impedance shows an inductive character because of the high resistance. This result is different from previous less-precise observations that showed a 1- to 2-percent inductive effect at the high frequency end (Reference 4). It is interesting to note that the electrodes in the present experiment have approximately the same surface area and separation as the electrodes in the previous experiment. Because of the capillary tube in the modified Jones cell, however, the cell constant is approximately an order of magnitude larger. If the observed inductance in the previous experiments was caused by some electrode process, it would explain the order of magnitude smaller inductive effect in the present

The Johns Hopkins University
APPLIED PHYSICS LABORATORY
Laurel, Maryland

Table 3

NaCl SOLUTION IMPEDANCE

08/13/84 14:57 NACL S=13.4PPT T=23.5C
KEY SETTINGS ARE A1B3C2D0F20H1I0M3P31S0T1

FREQUENCY PARASITIC BACKGROUND CAPACITANCE AND CONDUCTANCE
40K -3.23000000000E-17 -.000000000005

FREQUENCY PARASITIC BACKGROUND INDUCTANCE
10M 6.39600000000E-10

15:01 T=23.4

APPROXIMATE INDUCTANCE
-.0000000331

CELL CAPACITANCE
6.50000000000E-13

FREQUENCY (HZ)	VOLTAGE (VOLTS)	CURRENT (AMPS)	MEASURED IMPEDANCE MAGNITUDE (OHMS)	PHASE (DEG)	CORRECTED IMPEDANCE MAGNITUDE (OHMS)	PHASE (DEG)
1.0E+04	9.00E-01	1.10E-03	7.7227E+02	-0.04	7.7227E+02	-0.04
2.0E+04	8.90E-01	1.10E-03	7.7229E+02	-0.01	7.7229E+02	-0.01
4.0E+04	8.90E-01	1.10E-03	7.7215E+02	-0.01	7.7215E+02	+0.00
1.0E+05	8.90E-01	1.10E-03	7.7196E+02	-0.01	7.7196E+02	+0.01
2.0E+05	8.90E-01	1.10E-03	7.7169E+02	-0.00	7.7169E+02	+0.03
4.0E+05	8.90E-01	1.10E-03	7.7131E+02	+0.01	7.7131E+02	+0.08
1.0E+06	8.90E-01	1.10E-03	7.7112E+02	-0.04	7.7112E+02	+0.14
2.0E+06	8.80E-01	1.10E-03	7.7063E+02	-0.03	7.7062E+02	+0.33
4.0E+06	8.70E-01	1.10E-03	7.6952E+02	-0.09	7.6947E+02	+0.63
1.0E+07	7.50E-01	9.00E-04	7.7026E+02	-0.15	7.6994E+02	+1.65

15:03 T=23.4

APPROXIMATE INDUCTANCE
-.000000032

CELL CAPACITANCE
5.94000000000E-13

FREQUENCY (HZ)	VOLTAGE (VOLTS)	CURRENT (AMPS)	MEASURED IMPEDANCE MAGNITUDE (OHMS)	PHASE (DEG)	CORRECTED IMPEDANCE MAGNITUDE (OHMS)	PHASE (DEG)
1.0E+04	9.00E-01	1.10E-03	7.7031E+02	-0.04	7.7031E+02	-0.04
2.0E+04	8.90E-01	1.10E-03	7.7031E+02	-0.01	7.7031E+02	-0.01
4.0E+04	8.90E-01	1.10E-03	7.7022E+02	-0.01	7.7022E+02	+0.00
1.0E+05	8.90E-01	1.10E-03	7.7014E+02	-0.01	7.7014E+02	+0.00
2.0E+05	8.90E-01	1.10E-03	7.7002E+02	-0.01	7.7002E+02	+0.03
4.0E+05	8.90E-01	1.10E-03	7.6980E+02	+0.00	7.6980E+02	+0.07
1.0E+06	8.80E-01	1.10E-03	7.6970E+02	-0.04	7.6970E+02	+0.13
2.0E+06	8.60E-01	1.10E-03	7.6924E+02	-0.03	7.6923E+02	+0.30
4.0E+06	8.70E-01	1.10E-03	7.6821E+02	-0.09	7.6817E+02	+0.57
1.0E+07	7.50E-01	9.00E-04	7.6898E+02	-0.15	7.6872E+02	+1.50

The Johns Hopkins University
APPLIED PHYSICS LABORATORY
Laurel, Maryland

Table 4

NaCl SOLUTION IMPEDANCE

03/13/84 15:21 NACL S=50PPT T=23.7C
KEY SETTINGS ARE A4B3C2D0F11H1IOM3P31S0T1

FREQUENCY	PARASITIC BACKGROUND CAPACITANCE AND CONDUCTANCE	
40K	-2.500000000000E-17	.000000000000

FREQUENCY	PARASITIC BACKGROUND INDUCTANCE
10M	.000000000652

15:28 T=23.8C

APPROXIMATE INDUCTANCE
.000003014152

CELL CAPACITANCE
2.020000000000E-12

FREQUENCY (HZ)	VOLTAGE (VOLTS)	CURRENT (AMPS)	MEASURED IMPEDANCE MAGNITUDE (OHMS)	MEASURED IMPEDANCE PHASE (DEG)	CORRECTED IMPEDANCE MAGNITUDE (OHMS)	CORRECTED IMPEDANCE PHASE (DEG)
1.0E+04	7.00E-01	3.00E-03	2.3014E+02	-0.11	2.3014E+02	-0.11
2.0E+04	7.00E-01	3.00E-03	2.3002E+02	-0.05	2.3002E+02	-0.05
4.0E+04	7.00E-01	3.00E-03	2.2995E+02	-0.03	2.2995E+02	-0.02
1.0E+05	7.00E-01	3.00E-03	2.2995E+02	-0.02	2.2995E+02	+0.00
2.0E+05	7.00E-01	3.00E-03	2.2992E+02	-0.01	2.2992E+02	+0.03
4.0E+05	6.90E-01	3.00E-03	2.2985E+02	+0.01	2.2984E+02	+0.08
1.0E+06	7.00E-01	3.00E-03	2.2971E+02	+0.00	2.2971E+02	+0.17
2.0E+06	7.00E-01	3.00E-03	2.2953E+02	+0.05	2.2953E+02	+0.39
4.0E+06	6.90E-01	3.00E-03	2.2918E+02	+0.07	2.2916E+02	+0.74
1.0E+07	6.10E-01	2.60E-03	2.2930E+02	+0.22	2.2918E+02	+1.09

15:31 T=23.7C

APPROXIMATE INDUCTANCE
.000001411

CELL CAPACITANCE
1.920000000000E-12

FREQUENCY (HZ)	VOLTAGE (VOLTS)	CURRENT (AMPS)	MEASURED IMPEDANCE MAGNITUDE (OHMS)	MEASURED IMPEDANCE PHASE (DEG)	CORRECTED IMPEDANCE MAGNITUDE (OHMS)	CORRECTED IMPEDANCE PHASE (DEG)
1.0E+04	7.00E-01	3.00E-03	2.2957E+02	-0.11	2.2957E+02	-0.10
2.0E+04	7.00E-01	3.00E-03	2.2951E+02	-0.05	2.2951E+02	-0.05
4.0E+04	7.00E-01	3.00E-03	2.2947E+02	-0.03	2.2947E+02	-0.02
1.0E+05	7.00E-01	3.00E-03	2.2945E+02	-0.01	2.2945E+02	+0.00
2.0E+05	7.00E-01	3.00E-03	2.2942E+02	-0.01	2.2942E+02	+0.03
4.0E+05	6.90E-01	3.00E-03	2.2937E+02	+0.01	2.2937E+02	+0.07
1.0E+06	6.90E-01	3.00E-03	2.2933E+02	+0.00	2.2933E+02	+0.16
2.0E+06	7.00E-01	3.00E-03	2.2923E+02	+0.05	2.2923E+02	+0.37
4.0E+06	6.90E-01	3.00E-03	2.2894E+02	+0.07	2.2892E+02	+0.71
1.0E+07	6.10E-01	2.60E-03	2.2909E+02	+0.23	2.2898E+02	+1.81

The Johns Hopkins University
APPLIED PHYSICS LABORATORY
Laurel, Maryland

Table 5

SIMULATED SEAWATER SOLUTION IMPEDANCE

02/16/84 12:59 INSTANT SEA 35 PPT T=23.4
KEY SETTINGS ARE A4B3C2D0F11H1I0M3R31S0T1

FREQUENCY PARASITIC BACKGROUND CAPACITANCE AND CONDUCTANCE
40M 6.2C000000000E-17 -.000000000028

FREQUENCY PARASITIC BACKGROUND INDUCTANCE
10M 6.32600000000E-10

T=23.5C

APPROXIMATE INDUCTANCE
.000000012?4

CELL CAPACITANCE
1.24000000000E-12

FREQUENCY (HZ)	VOLTAGE (VOLTS)	CURRENT (AMPS)	MEASURED IMPEDANCE MAGNITUDE (OHMS)	MEASURED IMPEDANCE PHASE (DEG)	CORRECTED IMPEDANCE MAGNITUDE (OHMS)	CORRECTED IMPEDANCE PHASE (DEG)
1.0E+04	7.80E-01	2.20E-03	3.4419E+02	-0.05	3.4419E+02	-0.09
2.0E+04	7.80E-01	2.20E-03	3.4417E+02	-0.05	3.4417E+02	-0.04
4.0E+04	7.80E-01	2.20E-03	3.4415E+02	-0.03	3.4415E+02	-0.02
1.0E+05	7.80E-01	2.20E-03	3.4415E+02	-0.02	3.4415E+02	-0.00
2.0E+05	7.80E-01	2.20E-03	3.4413E+02	-0.01	3.4413E+02	+0.02
4.0E+05	7.70E-01	2.20E-03	3.4408E+02	+0.01	3.4407E+02	+0.07
1.0E+06	7.70E-01	2.20E-03	3.4405E+02	-0.01	3.4404E+02	+0.15
2.0E+06	7.70E-01	2.20E-03	3.4392E+02	+0.04	3.4391E+02	+0.34
4.0E+06	7.60E-01	2.20E-03	3.4351E+02	+0.04	3.4349E+02	+0.65
1.0E+07	6.70E-01	1.90E-03	3.4398E+02	+0.13	3.4383E+02	+1.67

23.7 C

APPROXIMATE INDUCTANCE
.000000012?4

CELL CAPACITANCE
1.?0000?000?0E-12

FREQUENCY (HZ)	VOLTAGE (VOLTS)	CURRENT (AMPS)	MEASURED IMPEDANCE MAGNITUDE (OHMS)	MEASURED IMPEDANCE PHASE (DEG)	CORRECTED IMPEDANCE MAGNITUDE (OHMS)	CORRECTED IMPEDANCE PHASE (DEG)
1.0E+04	7.80E-01	2.20E-03	3.4418E+02	-0.09	3.4418E+02	-0.09
2.0E+04	7.80E-01	2.20E-03	3.4411E+02	-0.04	3.4411E+02	-0.04
4.0E+04	7.80E-01	2.20E-03	3.4405E+02	-0.03	3.4405E+02	-0.02
1.0E+05	7.80E-01	2.20E-03	3.4402E+02	-0.02	3.4402E+02	-0.00
2.0E+05	7.80E-01	2.20E-03	3.4397E+02	-0.01	3.4397E+02	+0.03
4.0E+05	7.70E-01	2.20E-03	3.4389E+02	+0.01	3.4388E+02	+0.07
1.0E+06	7.70E-01	2.20E-03	3.4384E+02	-0.01	3.4384E+02	+0.15
2.0E+06	7.70E-01	2.20E-03	3.4369E+02	+0.04	3.4368E+02	+0.36
4.0E+06	7.60E-01	2.20E-03	3.4327E+02	+0.04	3.4324E+02	+0.68
1.0E+07	6.70E-01	1.90E-03	3.4372E+02	+0.13	3.4356E+02	+1.74

experiment. That is, the electrode process remained unchanged while the cell impedance was increased by an order of magnitude. Further, the relative changes in the impedance are essentially the same in the previous and present experiments.

Another set of measurements attempted to observe the Debye-Falkenhagen effect (Reference 3) that is observable within the frequency band of the LCR meter but at very low concentrations (around 1000 times less than seawater concentrations). Tables 6 and 7 show the results for 0.01-Molarity (M) solutions. The Debye-Falkenhagen effect is much stronger for $MgSO_4$ than for KCl; thus, a comparison can be made between the two tables. Within the accuracy of the measurements, no differences are observed and the corrected impedance is purely resistive. The concentration is too high to observe this effect.

Finally, much of the initial motivation to carry out these experiments was to measure the conductivity relaxation time. This number is at least 10^{-13} sec, which is based on the initial assumptions of Debye and Falkenhagen (Reference 3). Based on the experimental results of Table 5, the maximum seawater conductivity relaxation time, τ_c, is 5×10^{-10} sec. Therefore,

$$1 \times 10^{-13} < \tau_c < 5 \times 10^{-10} \text{ sec} \quad \text{or}$$

$$3.2 \times 10^{8} < f_c \left(= \frac{1}{2\pi\tau_c} \right) < 1.6 \times 10^{12} \text{ Hz}$$

3. PRESENT UNDERSTANDING OF THE ELECTRICAL PROPERTIES OF SEAWATER

The problem of understanding the electrical properties of seawater is a very complex one. This is because the detailed physics of electrolytic solutions is not completely understood and seawater is a heterogeneous solu-

Table 6

KCl SOLUTION IMPEDANCE

02/10/84 14:43 KCL .012M T=23.0
KEY SETTINGS ARE A4B3C2H0F1IH1I0M3R3S0T1

FREQUENCY PARASITIC BACKGROUND CAPACITANCE AND CONDUCTANCE
40K -6.00000000000E-17 .00000000006

FREQUENCY PARASITIC BACKGROUND INDUCTANCE
10M 6.50000000000E-10

14:54 T=23.8

APPROXIMATE INDUCTANCE
-.0000330528

CELL CAPACITANCE
2.19200000000E-13

FREQUENCY (HZ)	VOLTAGE (VOLTS)	CURRENT (AMPS)	MEASURED IMPEDANCE MAGNITUDE (OHMS)	MEASURED IMPEDANCE PHASE (DEG)	CORRECTED IMPEDANCE MAGNITUDE (OHMS)	CORRECTED IMPEDANCE PHASE (DEG)
1.0E+04	1.01E+00	0.00E+00	1.2899E+04	+0.01	1.2899E+04	+0.02
2.0E+04	1.00E+00	0.00E+00	1.2901E+04	+0.00	1.2901E+04	+0.02
4.0E+04	1.00E+00	0.00E+00	1.2900E+04	-0.01	1.2900E+04	+0.03
1.0E+05	1.00E+00	0.00E+00	1.2899E+04	-0.11	1.2899E+04	-0.01
2.0E+05	1.00E+00	0.00E+00	1.2895E+04	-0.17	1.2895E+04	+0.04
4.0E+05	1.00E+00	0.00E+00	1.2889E+04	-0.33	1.2889E+04	+0.08
1.0E+06	9.90E-01	0.00E+00	1.2885E+04	-0.86	1.2886E+04	+0.16
2.0E+06	9.50E-01	0.00E+00	1.2878E+04	-1.65	1.2883E+04	+0.38
4.0E+06	9.80E-01	0.00E+00	1.2899E+04	-3.34	1.2920E+04	+0.73
1.0E+07	8.70E-01	0.00E+00	1.3093E+04	-9.12	1.3257E+04	+1.27

The Johns Hopkins University
APPLIED PHYSICS LABORATORY
Laurel, Maryland

Table 7

MgSO4 SOLUTION IMPEDANCE

```
02/10/84 14:24 MgSO4 .01N T= 23.4C
KEY SETTINGS ARE      A4B3C2D0F1IH1I0M3R3ISOT1
++++++++++++++++++++++++++++++++++++++++++++++++++++++++++++++++++++++++++++++
FREQUENCY    PARASITIC BACKGROUND CAPACITANCE AND CONDUCTANCE
40K                    -6.800000000000E-17   -.000000000002
++++++++++++++++++++++++++++++++++++++++++++++++++++++++++++++++++++++++++++++
FREQUENCY    PARASITIC BACKGROUND INDUCTANCE
1UH                     .000000000973


14:32 T=23.6
++++++++++++++++++++++++++++++++++++++++++++++++++++++++++++++++++++++++++++++
APPROXIMATE INDUCTANCE
-.0000238102

CELL CAPACITANCE
 2.084000000000E-13
++++++++++++++++++++++++++++++++++++++++++++++++++++++++++++++++++++++++++++++
                                    MEASURED IMPEDANCE   CORRECTED IMPEDANCE
FREQUENCY VOLTAGE   CURRENT     MAGNITUDE    PHASE     MAGNITUDE    PHASE
  (HZ)    (VOLTS)   (AMPS)       (OHMS)     (DEG)       (OHMS)     (DEG)
1.0E+04   1.01E+00 0.00E+00   1.1209E+04   +0.01     1.1209E+04   +0.02
2.0E+04   1.00E+00 0.00E+00   1.1230E+04   +0.01     1.1230E+04   +0.02
4.0E+04   1.00E+00 0.00E+00   1.1249E+04   -0.01     1.1249E+04   +0.02
1.0E+05   1.00E+00 0.00E+00   1.1267E+04   -0.09     1.1267E+04   -0.01
2.0E+05   1.00E+00 0.00E+00   1.1282E+04   -0.13     1.1282E+04   +0.04
4.0E+05   1.00E+00 0.00E+00   1.1296E+04   -0.27     1.1297E+04   +0.07
1.0E+06   9.90E-01 0.00E+00   1.1313E+04   -0.72     1.1314E+04   +0.13
2.0E+06   9.90E-01 0.00E+00   1.1328E+04   -1.42     1.1331E+04   +0.28
4.0E+06   9.80E-01 0.00E+00   1.1359E+04   -2.91     1.1373E+04   +0.50
1.0E+07   8.30E-01 0.00E+00   1.1527E+04   -7.85     1.1634E+04   +0.83
```


The Johns Hopkins University
APPLIED PHYSICS LABORATORY
Laurel, Maryland

tion of many electrolytes. The importance of the electrical properties (i.e., dielectric and conductive) at radar frequencies has required some form of tabulation as a function of temperature, salinity, and frequency. This is currently done in a semi-empirical way using the formulas of Debye, and Cole and Cole (References 5 and 6) fitted to experimental data (Reference 7). The result is a reasonable representation of the true dielectric and conductive values of seawater as a function of temperature and salinity below 5 GHz. However, precision microwave radiometry requires equal precision of the known electrical properties of seawater. To improve the present semi-empirical formulas requires a greater understanding of the theory, including observed anomalous electrical properties. A brief review of the present understanding of the electrical properties of seawater and seawater-related electrolytes is presented in the following section.

3.1 Microwave Electrical Properties

Microwave data of the complex relative permittivity for electrolytic solutions is typically fitted to an equation of the form (Reference 7)

$$\varepsilon(\omega,T,S) = \varepsilon_\infty + \frac{\varepsilon_s(T,S) - \varepsilon_\infty}{1 + [j\omega\tau_D(T,S)]^{1-\alpha(T,S)}} - j\frac{\sigma(T,S)}{\omega\varepsilon_o} \quad (8)$$

where

T = temperature
S = salinity
ε_∞ = the relative dielectric constant at $\omega \gg 1/\tau_D$
ε_s = the static relative dielectric constant
ε_o = permittivity of free space [Farads/m]
ω = $2\pi f$, f = frequency in hertz
σ = conductivity [S/m]
τ_D = Debye relaxation time
α = empirical spreading parameter of relaxation times

The conductivity relaxation process is not represented by Equation (8) and neither are higher frequency resonances which impact ε_∞. However, since this model only claims agreement below 5 GHz, the details of the Debye and conductivity relaxations are not required. For example, for $\alpha = 0$ Equation (8) can be expanded to the form

$$\varepsilon(\omega,T,S) = \varepsilon_\infty + (\varepsilon_s - \varepsilon_\infty)\,(1 - (j\omega\tau_D) - (\omega\tau_D)^2 \text{---}) - j\,\frac{\sigma}{\omega\varepsilon_o} \qquad (9)$$

$$= \varepsilon_s - (\varepsilon_s - \varepsilon_\infty)\,(\omega\tau_D)^2 - j[(\varepsilon_s - \varepsilon_\infty)(\omega\tau_D) + \frac{\sigma}{\omega\varepsilon_o}]$$

Because $\omega\tau_D \ll 1$ below 5 GHz, this expansion will work very well. The expansion of any proper function would produce the same first-order structure. Thus, curve fitting data to Equation (8) at frequencies below 5 GHz will not definitively determine the true structure of the dielectric properties beyond 5 GHz. This fact is recognized by Klein and Swift (Reference 7).

In principle, ε_∞ and σ are functions of temperature, salinity, and frequency, and ε_S and τ_D are functions of temperature and salinity. A more general form of Equation (9) is given by

$$\varepsilon(\omega,T,S) = \varepsilon_\infty(\omega,T,S) + \frac{\varepsilon_s(T,S) - \varepsilon_\infty(\omega,T,S)}{1 + [j\omega\tau_D(T,S)]^{1-\alpha(T,S)}} \qquad (10)$$

$$- j\,\frac{1}{\omega\varepsilon_o}\,\frac{\sigma_{DC}(T,S)}{1 + j\omega\tau_C(T,S)}$$

where

σ_{DC} = DC conductivity

τ_c = conductivity relaxation time

The Debye relaxation process accounts for the damped rotation of the water molecule in the liquid state. The conductivity relaxation process accounts for the damped translational motion of the ionic charge carrier. Debye in 1913 (Reference 8) approximately determined the Debye relaxation time, τ_D, by considering Stoke's law converted for a rotating sphere and Brownian motion. The following formula was obtained.

$$\tau_D = \frac{8\pi\eta a^3}{kT} \tag{11}$$

where

η = viscosity of water

a = radius of water molecule

k = Boltzmann's constant

Surprisingly, this formula predicts reasonably well the observed relaxation time of water, which is on the order of 1×10^{-11} sec. Intuitively, the relaxation time of the translational motion of the ionic charge carriers in water should be similar to the rotational relaxation of the water molecule. Following a similar approach as Debye, the conductivity relaxation time can be approximately found by examining the charge density in light of Stoke's law and Brownian motion. The result is

$$\tau_C = \frac{6\pi\eta b x_o^2}{kT} \tag{12}$$

where

b = radius of charge carrier

x_o = 1/e point of Maxwell-Boltzmann distribution of charge density

Since

$$b \sim a$$

$$x_o \geq a$$

then

$$\tau_C \geq \tau_D$$

This result crudely verifies our intuition. It is interesting to note that the Debye-Falkenhagen computation of the conductivity relaxation time is based on the velocity or mobility part of the conductivity and does not include the random motion of the ion.

The real and imaginary parts of the general complex permittivity [Equation (10)] are for $\alpha = 0$, thus

$$\varepsilon = \varepsilon' - j\varepsilon'' \tag{13}$$

$$\varepsilon' = \varepsilon_\infty + \frac{\varepsilon_S - \varepsilon_\infty}{1 + (\omega\tau_D)^2} - \frac{\sigma_{DC}\,\tau_C/\varepsilon_o}{1 + (\omega\tau_C)^2} \tag{14}$$

$$\varepsilon'' = \frac{(\varepsilon_S - \varepsilon_\infty)\omega\tau_D}{1 + (\omega\tau_D)^2} - \frac{\sigma_{DC}\,\tau_C/\varepsilon_o\omega}{1 + (\omega\tau_C)^2} \tag{15}$$

Figures 5a and 5b are plots of ϵ' and ϵ'', respectively, for different values of τ_c. The cases for $\tau_c = \tau_D$ or 0 are the same curves. Interestingly, with $\tau_c = \tau_D$ the conductivity effects cannot be differentiated from the case of $\tau_c = 0$. However, for $\tau_c/\tau_D = 0.5$ and 2 there are observable differences. If $\tau_c \sim \tau_D$ (it is unlikely that they are exactly equal) then the conductivity relaxation effect is an important term in the complex permittivity formula. The efforts to model the permittivity beyond 5 GHz would then be helped by including this effect.

Figures 6a and 6b illustrate the dielectric properties of pure water. Figure 6a also shows typical skin depth attenuation of seawater (References 9 and 10). The pure water spectra show a fair amount of structure. The hump at 20 GHz is the Debye relaxation phenomenon. The two peaks between 10^{12} and 3×10^{13} Hz are called the hindered translation, ν_T, and librational band, ν_L, respectively. They are caused by H_2O and H_2O (i.e., dimmer-like) interactions (Reference 11). Most of the higher frequency peaks are caused by the internal motion of the water molecule (i.e., rotation vibration (Reference 11). Beyond the Debye relaxation, the complex permittivity is represented by ϵ_∞. It is dominated by these infrared resonances. This can be seen by examining the real part of $\epsilon_\infty (= \epsilon'_\infty - j\epsilon''_\infty)$;

$$4.9 > \epsilon'_\infty > 1.69 > 1$$
Microwave Optical

ϵ_∞ is determined by resonances and relaxations beyond the frequency of interest. Based on the above relationship, the microwave region is heavily influenced by the infrared resonances.

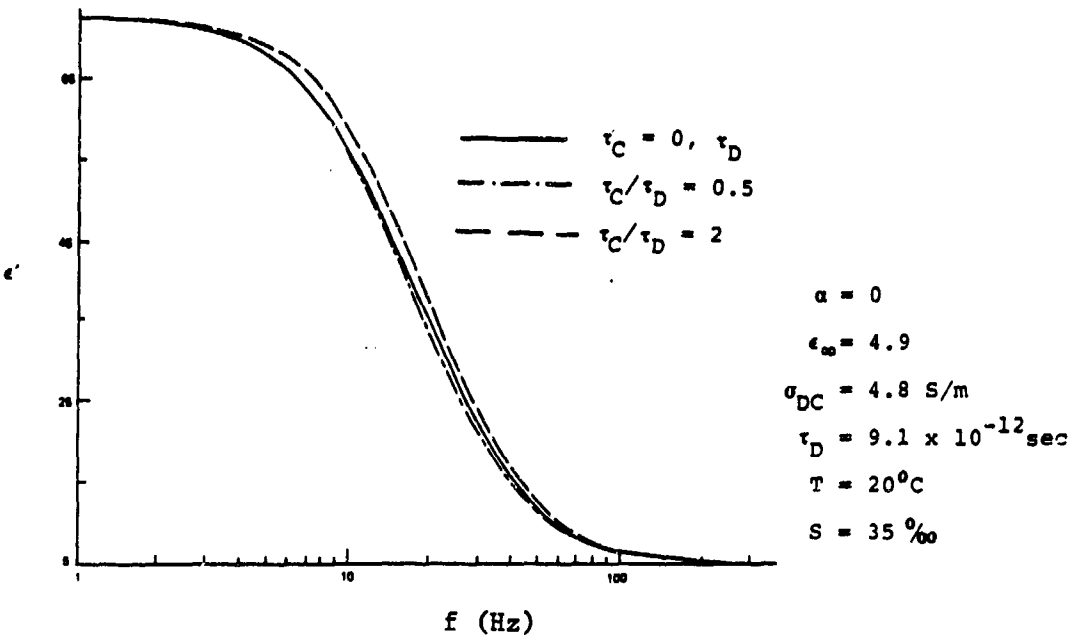

Figure 5(a) Real Part of the Permittivity Versus Frequency

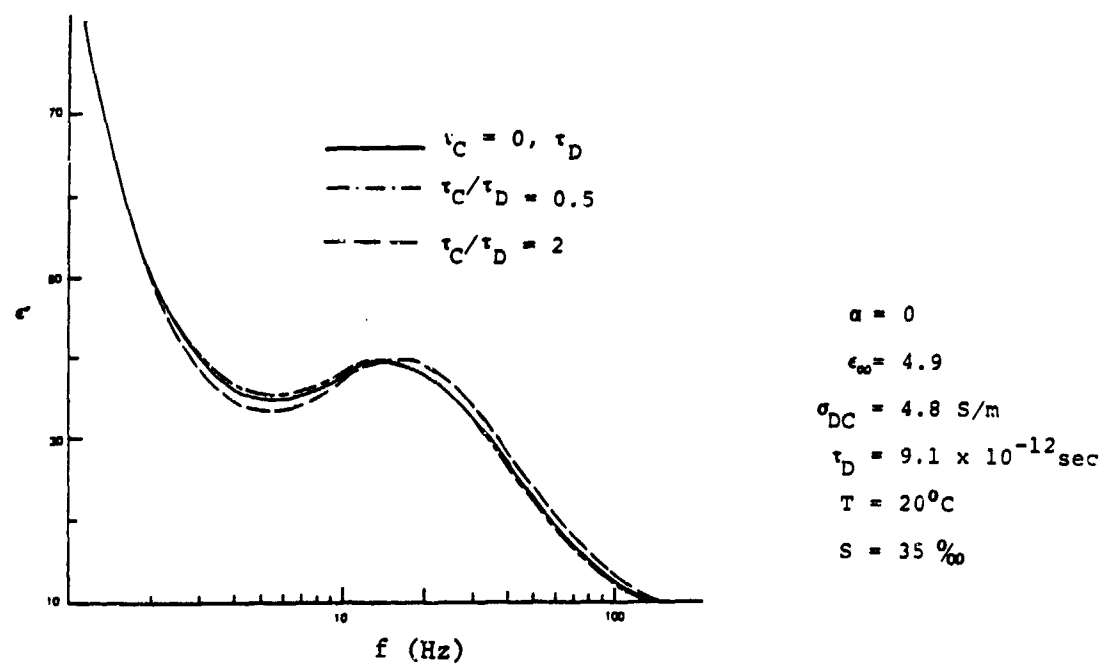

Figure 5(b) Imaginary Part of the Permittivity Versus Frequency

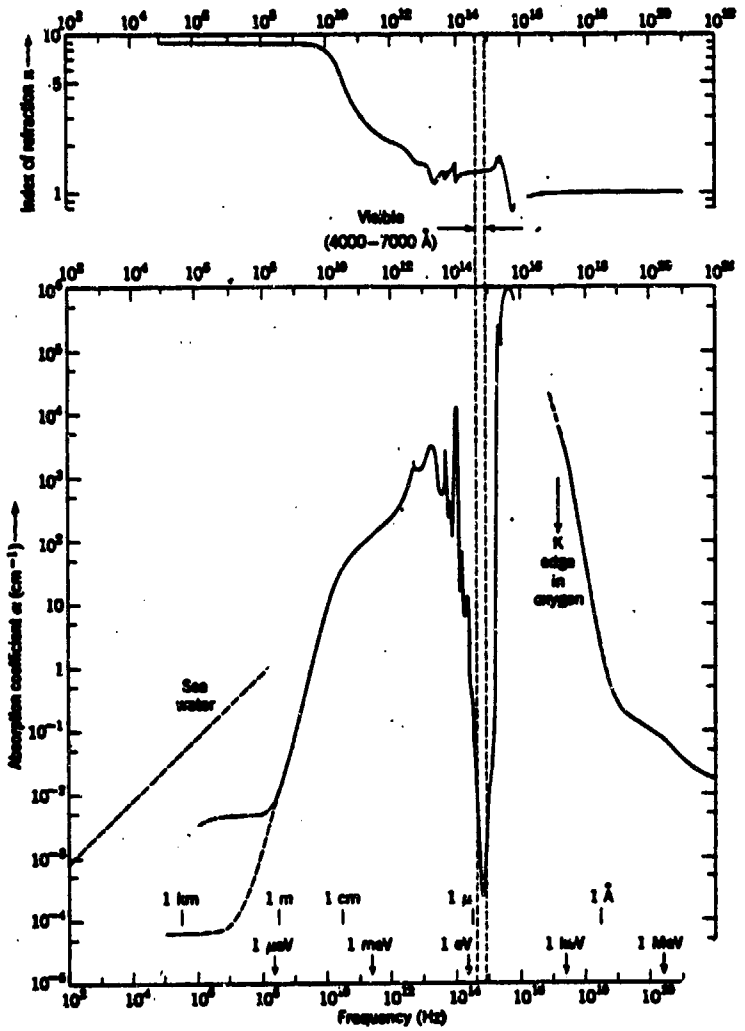

Note: Also shown as abscissas are an energy scale (arrows) and a wavelength scale (vertical lines). The visible region of the frequency spectrum is indicated by the vertical dashed lines. The absorption of coefficient for seawater is indicated by the dashed diagonal line at the left. Scales are logarithmic in both directions.

Figure 6(a) The Index of Refraction (top) and Absorption Coefficient (bottom) for Liquid Water as a Function of Linear Frequency

The Johns Hopkins University
APPLIED PHYSICS LABORATORY
Laurel, Maryland

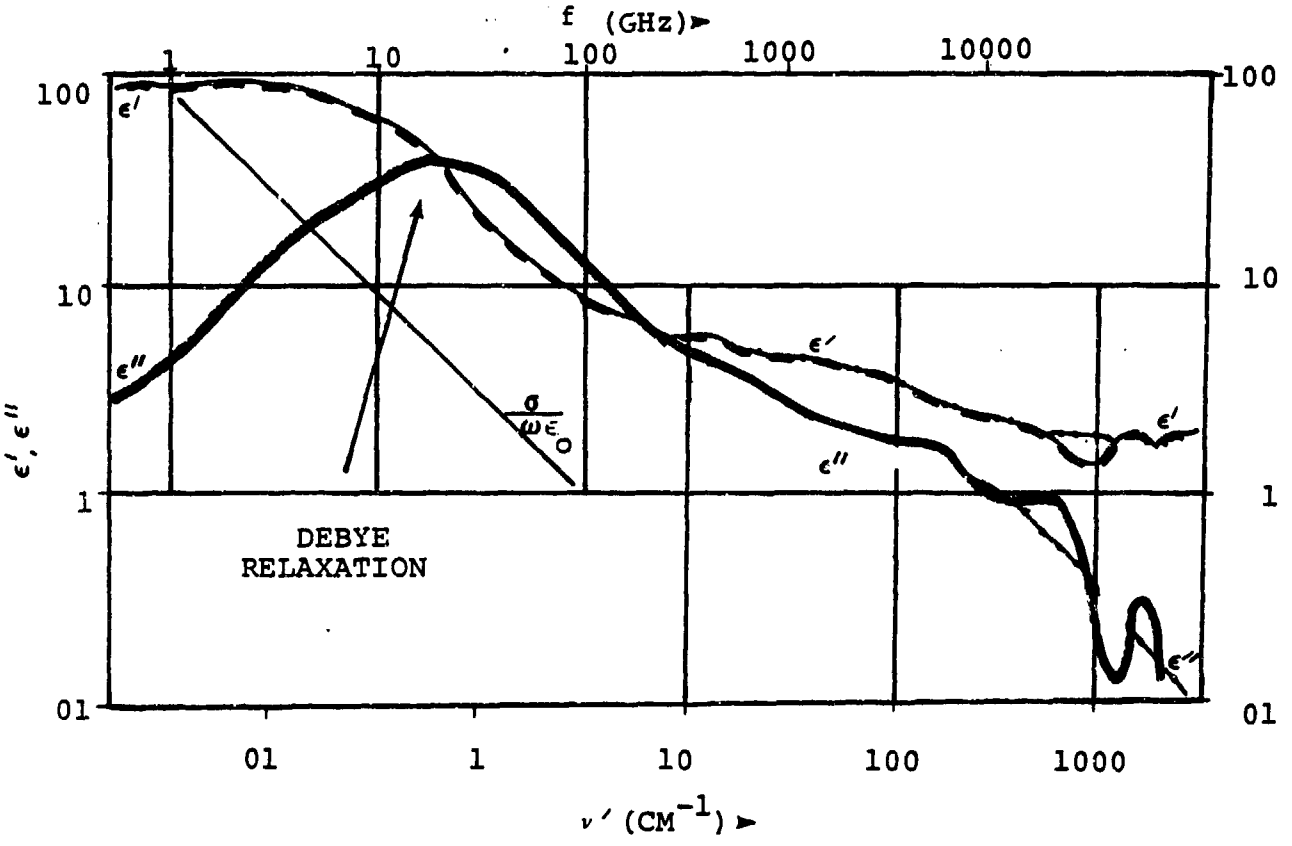

Figure 6(b) Logarithmic Plot of ε' (dashed line), ε'' (solid line) and $\sigma/\omega\varepsilon_0$ (solid line) Against Frequency ν (wavenumber ν') for 20°C and σ = 5 S/m

The presence of a solute does influence ε_∞. This is demonstrated by Figure 7, which shows experimental data of the ν_L and ν_T band of pure D_20 and D_20 KCl and NaCl solutions at 4 Molarity (M). The solutions are highly concentrated compared to seawater but do show significant changes in the spectrum. This will directly impact ε_∞ at microwave frequencies and make it a function of salinity. It is also well know (Reference 11) that these bands are sensitive to temperature. Thus ε_∞ is indeed a function of frequency, salinity, and temperature.

The relaxation time spreading parameter, α, is not zero and is thought to be a function of temperature and salinity (References 12 and 13). This is illustrated in Figure 8 for H_20 solutions of NaCl. The precise nature of α will not be understood until the conductivity relaxation effects are understood. The relaxation time spreading parameter influences the falloff of the Debye relaxation. As illustrated by Figures 5a and 5b, the conductivity relaxation process also influences the falloff of the curves. Thus, these two different yet similar effects may be difficult to separate.

3.2 Anomalous Electrical Properties

In addition to well-understood physical mechanisms that impact seawater electrical properties, there are reported observations of anomalous behavior of solutions of single electrolytics which compose seawater. These are listed below (Reference 13).

(1) Anomalously high conductivity of electrolytic solutions at concentrations close to seawater at 582 MHz (Reference 14).

(2) Additional relaxation phenomena at submillimeter wavelengths. The dielectric constant is modelled as

The Johns Hopkins University
APPLIED PHYSICS LABORATORY
Laurel, Maryland

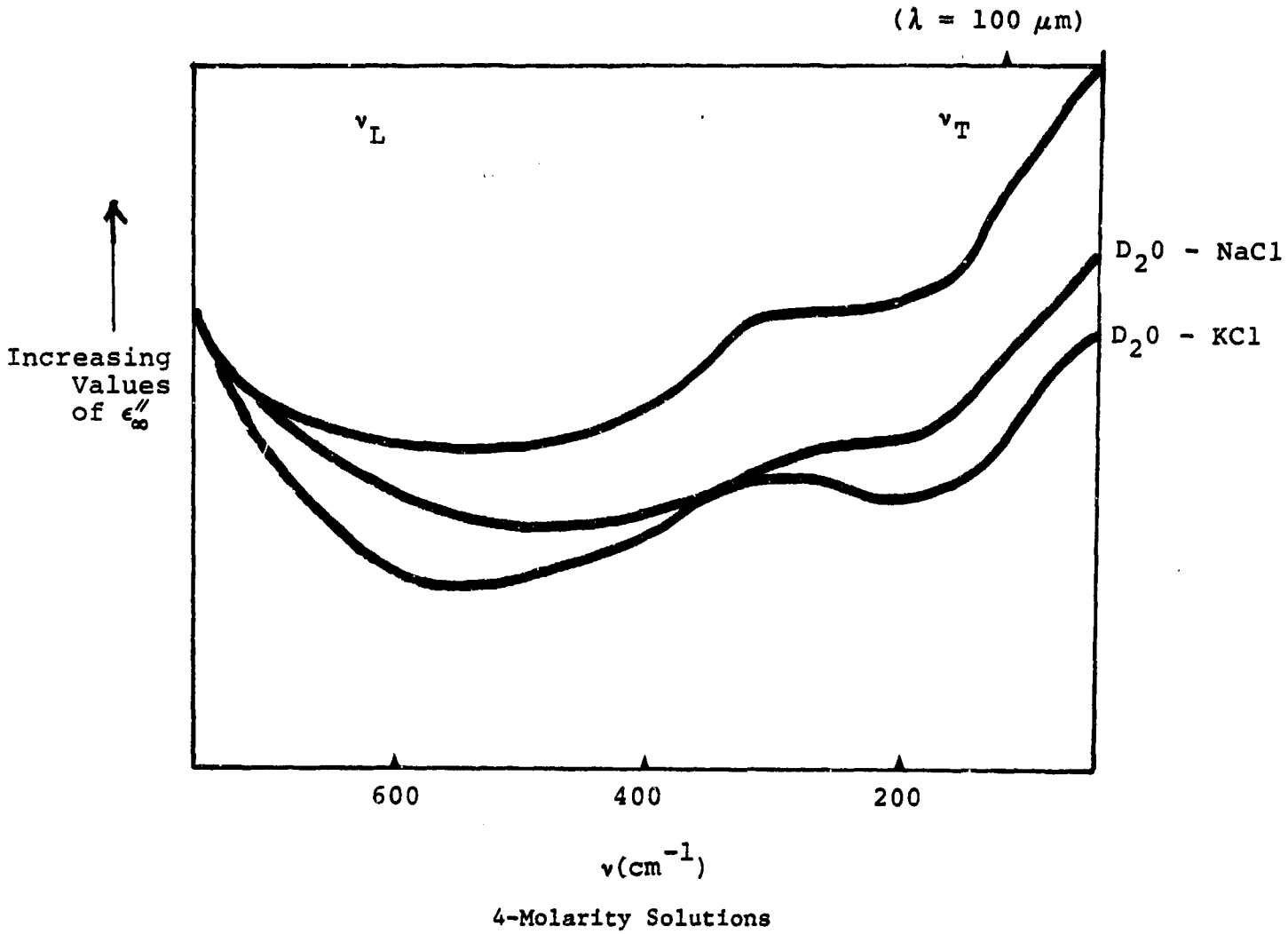

Figure 7 Experimental Data of the ν_L and ν_T Band of Pure D_2O and D_2O KCl and NaCl Solutions at 4-Molarity Concentration

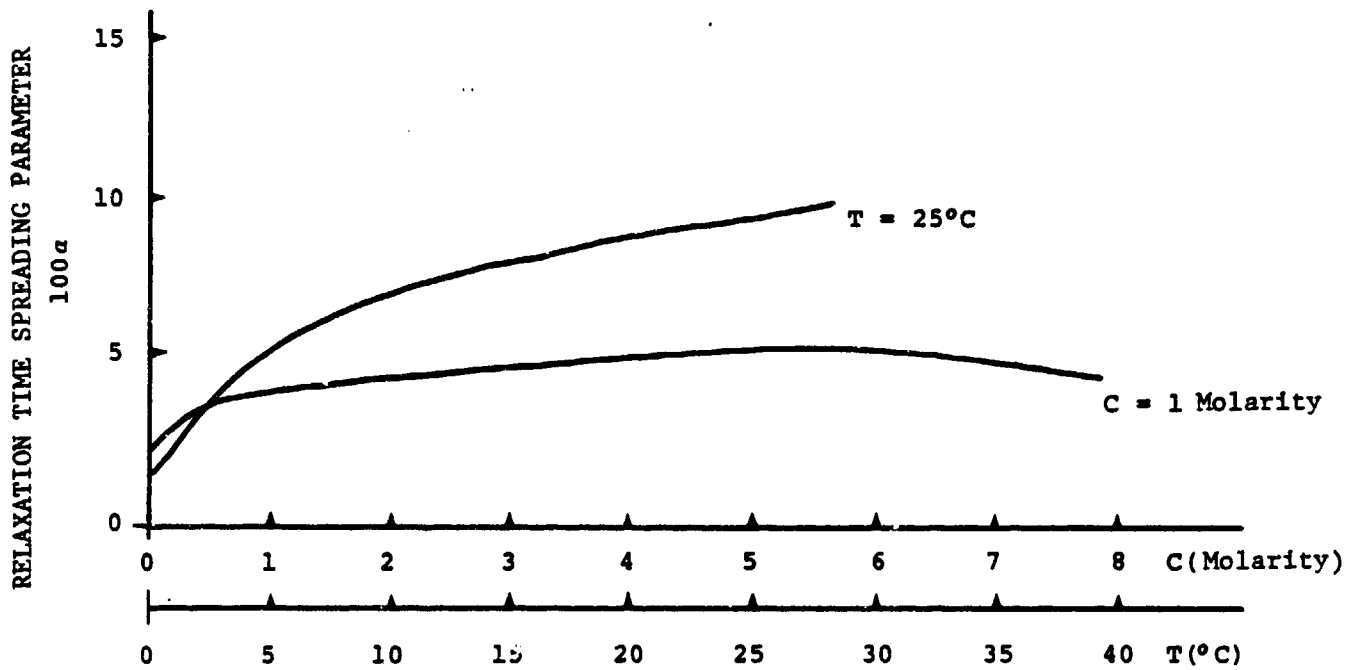

Figure 8 Relaxation Time Spreading Parameter, α, as a Function of Temperature (constant concentration c = 1 Molarity) and Concentration (constant temperature T = 25°C) for a Water-NaCl Solution

$$\epsilon = n^2 + \frac{\epsilon_{\infty} - n^2}{1 + j\omega\tau_2} \qquad \frac{\epsilon_s - \epsilon_{in}}{1 + (j\omega\tau)^{1-\alpha}}$$

where τ_2 is the additional relaxation time.

4. CONCLUSIONS

The electrical properties of seawater have been examined with particular emphasis on the effects of relaxation of the charge carriers with the frequency of the applied field. Such effects have not been definitively quantified either experimentally or theoretically. Experiments conducted were not conclusive. It is possible that the conductivity relaxation time (the characteristic time its takes a translating charge carrier to relax back to equilibrium) is similar to the Debye relaxation time (the characteristic time it takes a rotating molecule to relax back to equilibrium in a fluid or solid), making direct observation of this effect difficult. The conductivity relaxation time has been constrained to be within $5 \times 10^{-10} > \tau_c > 1 \times 10^{-13}$ sec. It is quite possible that $\tau_c \sim \tau_D$ since the dampening mechanisms should be similar. If this is true, the dielectric models will need to include the effects of conductivity relaxation. Also, it is recognized that resonant far-infrared (including submillimeter) bands can influence the dielectric properties at and above 40 GHz.

A more definitive impedance experiment attempting to measure the conductivity relaxation time will require the following:

- A test cell with a much larger cell constant
- Impedance measurements at frequencies close to 1 GHz
- A high degree of precision or a means of nulling the DC resistance of the electrolytic solution

Also, the development of a reasonable theory may aid in the selection of a more optimal temperature and salinity of the samples.

The Johns Hopkins University
APPLIED PHYSICS LABORATORY
Laurel, Maryland

REFERENCES

1. Condon, E. U. and Odishow, H. (Editors), Handbook of Physics, 2nd Edition, McGraw-Hill Book Co. (1967) p. 4-77.

2. Jackson, J. D., Classical Electrodynamics, John Wiley & Sons, Inc., 1962, p. 225.

3. Debye, P. and Falkenhagen, H., Physik. Z., 29, 121, 401 (1928); H. Falkenhagen, Electrolytes, Clarendon Press, (1934), p. 169.

4. Kolbeck, J. B., "Excitation Frequency Dependence of Conductivity of Electrolytic Solutions," M. S. Thesis, The Naval Postgraduate School, June 1983.

5. Debye, P., Polar Molecules, Dover Reprint, originally published by Reinhold Publishing Corp., 1929.

6. Cole, K. S. and Cole, R. H., J. Chem. Phys., 9, pp. 341-351, 1941.

7. Klein, L. A. and Swift, C. T., IEEE Trans. Antennas Propagat., AP-25 No. 1, pp. 104-111, January 1977.

8. Debye, P. Berichte der Deutschen Physikalishchen Gesellshaft, Vol. 15, No. 16, pp 777-793 (1913)

9. Jackson, J. D., Classical Electrodynamics, 2nd Edition, Wiley & Sons, Inc., (1975), p. 291.

10. Franks, F. Editor, Water A Comprehensive Treatise, Vol. 1, The Physics and Physical Chemistry of Water, Plenum Press, 1972, Chapter 7, p. 295.

11. Eisenberg, D. and Kauzmann, W., The Structure and Properties of Water, Oxford University Press (1969).

12. Draegert, D. A. and Williams, D., J. Chem. Phys. 48, 401-407, January 1968.

13. Hasted, J. B., Aqueous Dielectrics, Chapman and Hall (1973).

14. Hasted, J. B. and Roderick, G. W., J. Chem. Phys., 29 17 (1958)

EXTERNAL DISTRIBUTION for STD-R-1071

Chief of Naval Research
800 North Quincy Street
Arlington, VA 22218
ATTN: Code 422CS

Chief of Naval Research
800 North Quincy Street
Arlington, VA 22218
ATTN: Code 425AR

Commanding Officer
Naval Research and Development Activity
NSTL Station
Bay Saint Louis, MS 39529
ATTN: Code 335

Director
Naval Research Laboratory
Washington, DC 20375
ATTN: Code 2627

Commanding Officer
Naval Research Laboratory
Washington, DC 20375
ATTN: Code 4006

Commanding Officer
Naval Research Laboratory
Washington, DC 20375
ATTN: Code 4344

Commanding Officer
Naval Research Laboratory
Washington, DC 20375
ATTN: Code 7913P

Commanding Officer
Naval Plant Representative Office
Johns Hopkins Road
Laurel, MD 20707
ATTN: Administrative Contracting Officer

Allied/Amphenol Prod.
Bendix Electr. Components Div.
40-60 Delaware Street
Sidney, NY 13838
ATTN: Paul I. Pressel

EXTERNAL DISTRIBUTION for STD-R-1071 (Contd)

Center for Radar Astronomy
Stanford University
233 Durand
Stanford, CA 94305
ATTN: Dr. John F. Vesecky

Defense Technical Information Center
Bldg. 5, Cameron Station
Alexandria, VA 22314

Electrical Engineering Department
University of Maryland
College Park, MD 20740
ATTN: Dr. Robert O. Harger

Environmental Research Institute of Michigan
P.O. Box 8618
Ann Arbor, MI 48107
ATTN: Dr. R. A. Shuchman

Max-Planck Institute for Meteorology
Bundesstrasse 55
D-2000 Hamburg 13
Fed. Rep. Germany
ATTN: Prof. Dr. Klaus Hasselmann

The University of Kansas Center Research, Inc.
2291 Irving Hill Drive, Campus West
Lawrence, KS 66045-2969
ATTN: Dr. Richard K. Moore

Dr. Omar H. Shemdin
727 Georgian Road
La Canada, CA 91011